

## Particle charge evolution during acceleration processes in solar flares

M D Rodríguez-Frías<sup>†</sup>, L del Peral<sup>†</sup> and J Pérez-Peraza<sup>‡</sup>

<sup>†</sup> Departamento de Física, Universidad de Alcalá, 28871 Alcalá de Henares, Madrid, Spain

<sup>‡</sup> Instituto de Geofísica, UNAM, 04510-CU, México DF, Mexico

Received 7 June 1999, in final form 16 November 1999

**Abstract.** It has been customary to assume that the charge state of energetic particles corresponds to the ionization equilibrium of the ambient plasma within the acceleration region. Nonetheless, we ascribe to a different opinion, by suggesting that charge interchange mechanisms may be activated during the ensuing acceleration process. We substantiate our claim by the calculated behaviour of charge states corresponding to energized ions while they are accelerated in the source regions. These computations are based on the electron capture and loss cross sections. Results from the analysis allow us to conclude that, contrary to the general assumption, charge exchange processes may be invoked during the acceleration of energized ions in solar flares.

### 1. Introduction

It is usually assumed that the charge state of cosmic rays corresponds to the ionization equilibrium of the plasma where they undergo acceleration (i.e. solar corona at  $T \sim 1.6 \times 10^6$  K) [1]. Based on this assumption, the hypothesis commonly found in the literature is that the charge exchange processes involving particles and the source matter, are not established during the acceleration process or subsequent propagation, consequently, particles preserve their original charge states without interaction with the source, following the semi-empirical parametrization of Barkas–Blume:

$$q^* = Z[1 - \xi \exp(-b\beta/\alpha Z^{2/3})] \quad (1)$$

where  $q^*$  is the ion effective charge,  $\beta$  is the ion velocity relative to the speed of light,  $\alpha$  is the fine-structure constant,  $b = 0.93$  and  $\xi$  is a temperature-dependent parameter. At laboratory scales  $\xi = 1$ , while for an astrophysical plasma at temperature  $T$ ,  $\xi = \exp(-130kT/mc^2)$ .

If such is the case, why then, are the charge state values predicted by the semi-empirical expression of Barkas–Blume lower than the experimental ones, and why were the measured charge states of iron ions in the energy range 10–150 keV/nucleon recorded during the May 14, 1974 event between +13 and +14, whereas at higher energies charge states up to +18 were detected? Finally, why do the mean charge states of iron ions at  $E \sim 0.2$  MeV/nucleon for different events vary from +11 up to +26, and in an analogous way at  $E \sim 2$  MeV/nucleon for similar events? [2–4].

Intrigued by these ambiguities we have decided to investigate the conditions that account for the charge exchange, in order to determine whether particles maintain their local charge states during the acceleration or trade-in for another.

The charge states of energized ions and their evolution as they traverse through matter is a very important factor to consider during the investigations of particle interaction with

matter and electromagnetic fields. At the laboratory level, the study of the stopping powers of ions as they travel through different kinds of materials is strongly dependent on an accurate knowledge of equilibrium charge states. In cosmic ray physics, it is also very important to determine stopping powers in different contexts: evaluation of the radiation fluxes resulting from the interaction of particles with matter and magnetic fields, generation of secondary nuclei by spallation, modulation of low-energy ions in the heliosphere and magnetosphere boundaries, and finally, whenever magnetic fields are present, because the magnetic rigidities of ions are dependent on their charge states during the acceleration and escape from the source.

## 2. Cross sections for charge exchange processes

Energized ions travelling inside a plasma at velocity  $v$  may undergo two charge exchange processes. They can capture or lose electrons while they interact with the ambient plasma. Therefore, the following processes have to be considered: electron ionization, autoionization after electron excitation, radiative recombination and dielectronic recombination. However, most experimental cross sections for charge exchange processes have only been obtained at the laboratory level, usually limited to specific ions (mostly hydrogenics or fully stripped) and a few atomic targets at very restricted velocity ranges. This is due to the theoretical analytical formalisms propagated throughout literature that always considered them as motionless targets. In contrast, at the astrophysical level the ambient temperature exhibits a wide range of variation and becomes a crucial factor which must be accounted for. Therefore, in this paper, we have quantified temperature-dependent cross sections for charge exchange processes by considering the thermal velocity of electrons in the plasma, averaging the respective cross sections over the thermal electron distribution. This improvement has allowed us an update of the charge exchange cross section status.

The cross sections for electron radiative capture by a fast ion, with effective charge  $q$  and velocity  $v$ , have been taken from Bethe and Salpeter [5] and Nikolaev [6]. For dielectronic recombination the cross section is calculated using the expression given by Burgess [7]. Finally, electron ionization and autoionization have been calculated following Arnaud and Rothenflug [8]. We have proceeded as Pérez-Peraza *et al* [9], by adapting the charge exchange cross sections to fit a continuous description throughout the whole range of solar energized ions and introducing, instead of the ion velocity, a relative velocity between the ion and the target's thermal velocity.

Consequently, we have followed the same steps as in the radiative capture mechanism, in order to introduce the thermal velocity of the targets. From these calculations we have obtained a global description of charge exchange cross sections for any kind of target, highly charged hydrogenic and fully stripped projectiles, within a wide range of temperatures and ion velocities.

Based on the results obtained we can state that capture cross sections are greater for highly ionized projectiles in all the kinetic energy range studied, while for the ionization cross section, the opposite behaviour is found. The increase of the plasma temperature translates into an increase of the radiative capture cross section, while the opposite phenomenon holds true for the electron ionization loss cross section. We can finally state that, in the low ion velocity region, capture predominates over ionization processes. This situation persists while the particle accelerates from thermal velocity until it reaches an intermediate velocity. At this velocity both cross sections equalize. While for higher ion velocities the ionization becomes the overwhelming process.

### 3. The charge state behaviour under acceleration mechanisms

Here, our analysis is focused on projectile ions accelerated from the background thermal matter, in such a way that their initial velocities and charge states correspond to those of the thermal plasma. For the thermal charge states,  $q_{th}$ , we rely merely on calculations based on astrophysical plasma ionization fractions given by Arnaud and Rothenflug [8].

Particles traversing through matter generally lose energy due to Coulomb collisions with the electrons of the medium, where the Bethe–Bloch equation gives the energy loss rate. If an acceleration mechanism does not interfere, the energy loss will bring the particle to thermalize. Nevertheless, if an acceleration mechanism is present, it will transfer energy to the given particle at the rate

$$\left(\frac{dE}{dt}\right)_{acc} = \alpha E^\eta \quad (2)$$

where  $\alpha$  is the acceleration efficiency and  $\eta$  depends on the acceleration mechanism. The two mechanisms under consideration are the Fermi (F) and betatron (b) mechanisms.

The stopping and acceleration effects balance when the Bethe–Bloch relation and (2) have the same value. Consequently, the critical efficiencies,  $\alpha_{cF}$  and  $\alpha_{cb}$  ( $s^{-1}$ ), for effective ion acceleration in a plasma under Fermi and betatron acceleration mechanisms respectively, can be deduced [10]:

$$\alpha_{cF} = 3.89 \times 10^{-7} Z_t \frac{n_t^{0.98}}{T^{0.96}} \left(\frac{q^{1.92}}{A^{0.88}}\right) \quad (3)$$

$$\alpha_{cb} = 0.28 Z_t \frac{n_t^{0.97}}{T^{1.45}} \left(\frac{q^{1.87}}{A^{0.67}}\right) \quad (4)$$

where  $q$  is the ion effective charge,  $n_t$  ( $cm^{-3}$ ) is the target density number of the source,  $Z_t$  is the charge of the target ions,  $A$  is the mass number and  $T$  is the temperature of the plasma. Therefore, when the efficiency of the acceleration mechanism is higher than the critical efficiency, the Coulomb energy loss is lower than the acceleration rate and the ion is energized, while the opposite behaviour is found for acceleration efficiencies lower than the critical efficiency.

Once the acceleration condition is fulfilled, the ion is accelerated from the thermal matter, starting with an averaged thermal effective charge  $q_{th}$ . While the ion is accelerated, the effective charge state,  $q_{th}$ , evolves iteratively in each acceleration step, according to the equation

$$q^* = q_0 + n_t t_a \Delta q_i \int_0^c [\sigma_{ioniz}(v)] v f(v) dv - n_t t_a \Delta q_c \int_0^c [\sigma_{capture}(v)] v f(v) dv \quad (5)$$

where  $q_0$  is the effective charge of the ion at the beginning of each acceleration step expressed in electron charge units (for the first acceleration step  $q_0 = q_{th}$ ),  $\Delta q_i$  and  $\Delta q_c$  are the average charge exchange in each ionization and capture process respectively,  $f(v)$  is the electron distribution which is a Maxwellian in the rest frame of the plasma,  $\sigma_{ioniz}$  is the total cross section for electron loss,  $\sigma_{capture}$  is the total cross section for electron capture and  $t_a$  is the time spent in the acceleration step that can be written, respectively, for the Fermi and betatron acceleration mechanisms as

$$t_a^F = \frac{2}{\sqrt{2\mu c^2 \alpha_F}} \left(\sqrt{E_f} - \sqrt{E_i}\right) \quad (6)$$

$$t_a^b = \frac{1}{2\alpha_b} \ln\left(\frac{E_f}{E_i}\right) \quad (7)$$

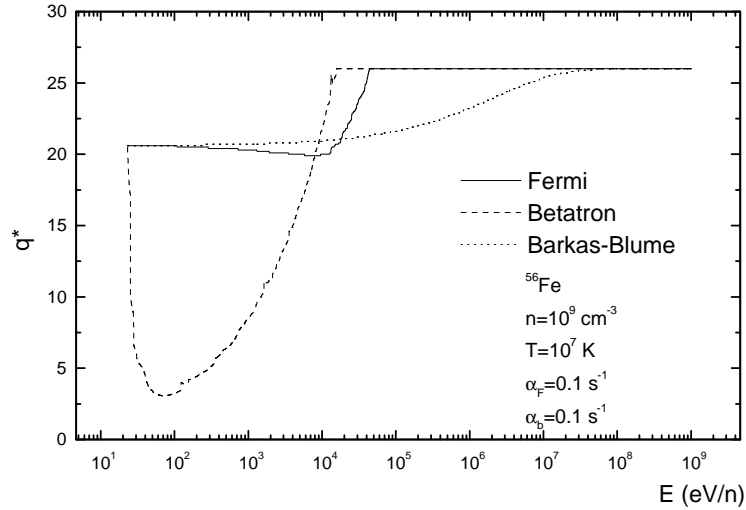


**Figure 1.** Dependence of the effective charge,  $q^*$ , of  $^{56}\text{Fe}$  ions with the energy under Fermi and betatron acceleration mechanisms. Semi-empirical calculations with the Barkas–Blume formula are given for comparison when no acceleration process is acting.

where  $E_i$  and  $E_f$  are the initial and final kinetic energies of the ion for each acceleration step,  $\alpha_b$  and  $\alpha_F$  are the betatron and Fermi acceleration efficiencies, and  $\mu$  is the nucleon mass.

Figure 1 shows the results of the average effective charge of fast  $^{56}\text{Fe}$  ions being accelerated in an ionized hydrogen source, typical of coronal impulsive flare conditions ( $T = 10^7$  K;  $n_i = 10^9$  cm $^{-3}$ ), under two different mechanisms, Fermi and betatron, assuming that their respective acceleration efficiencies are  $10^{-1}$  s $^{-1}$ . We have followed the acceleration process up to 1 GeV for the ions, independently of the trapping time needed. Additionally, the evolution of the effective charge obtained with the semiempirical parametrization of Barkas–Blume is presented for comparison, and due to the fact that the acceleration mechanism has not been taken into account in this parametrization, the ions do not enter the electron capture region but directly undergo complete ionization. Full ionization is reached quicker when the acceleration mechanism is acting.

The ion begins the process in the thermal equilibrium charge state, in the region dominated by electron capture, hence the ion captures electrons and accelerates. Two situations are then possible. First, when the acceleration rate is not sufficiently high, the ion thermalizes before it can reach the velocity region where the electron loss predominates over electron capture. In such a case, the ion loses its energy and finally becomes thermal. In contrast, when the acceleration rate is high enough the ion surpasses the capture stage and thus avoids thermalization. Therefore, it becomes stripped because the electron loss process predominates over electron capture. Depending on its trapping time within the source, the ion finally assumes a specific charge state. As was previously mentioned, in the first case, ions cannot escape from the source and hence, no accelerated ions to be considered in the study may be obtained. In the second instance, however, the ions acquire an effective charge depending on the acceleration mechanism and the time they remain in the acceleration region. These two factors nevertheless are liable to change from one acceleration region to another.

The effective charge of the particles versus the energy by nucleon of iron, calcium and silicon fast ions are presented in figure 2. The two acceleration mechanisms considered are

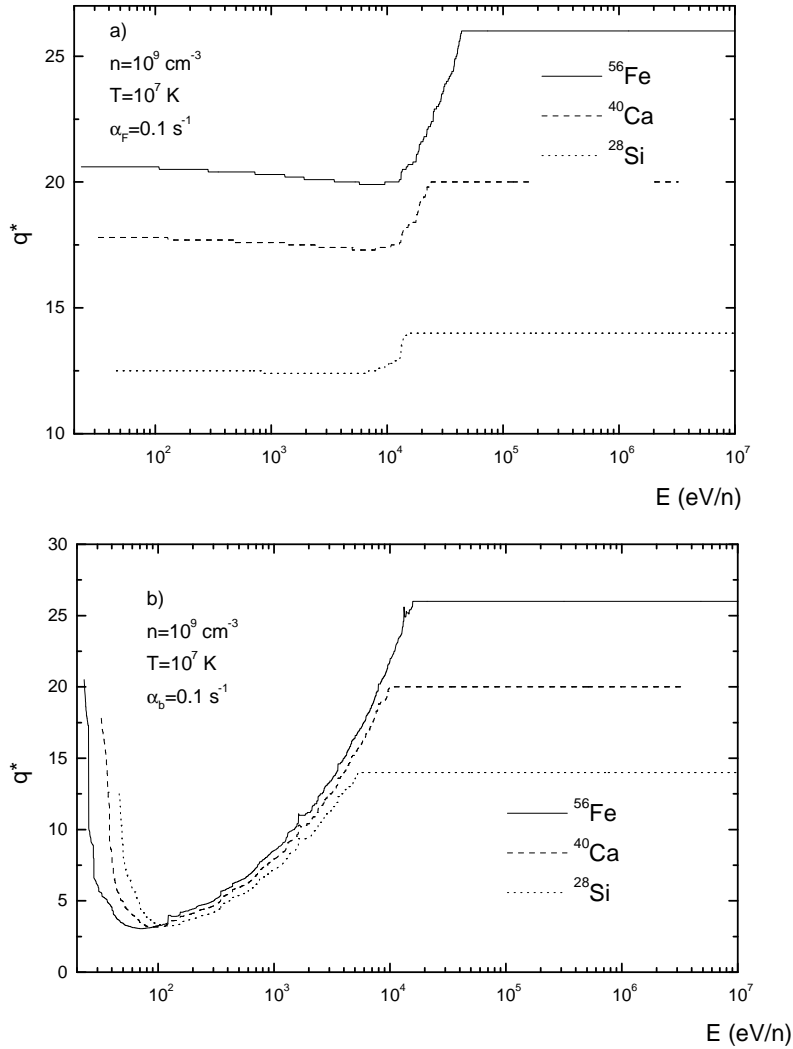


**Figure 2.** Effective charge,  $q^*$ , of  $^{56}\text{Fe}$ ,  $^{40}\text{Ca}$  and  $^{28}\text{Si}$  fast ions versus the kinetic energy under Fermi (a), and betatron (b), acceleration mechanisms with  $0.1 \text{ s}^{-1}$  acceleration efficiency in a  $10^7 \text{ K}$  hot plasma and  $10^9 \text{ cm}^{-3}$  density number.

Fermi (a) and betatron (b), with  $0.1 \text{ s}^{-1}$  acceleration efficiency in a  $10^7 \text{ K}$  hot plasma with  $10^9 \text{ cm}^{-3}$  density number.

Figure 3 presents the evolution of the effective charge with the trapping time in the plasma source. Under the betatron acceleration mechanism (b), the projectile starts capturing electrons faster than with the Fermi acceleration mechanism (a). In addition, the capture rate of electrons is higher for the betatron mechanism. The effective charge evolution of the ions, when the electron loss process is taking place, is also different for each mechanism, as can be seen from figure 3. Finally, the projectile becomes fully ionized, its ionization being quicker under the betatron mechanism.

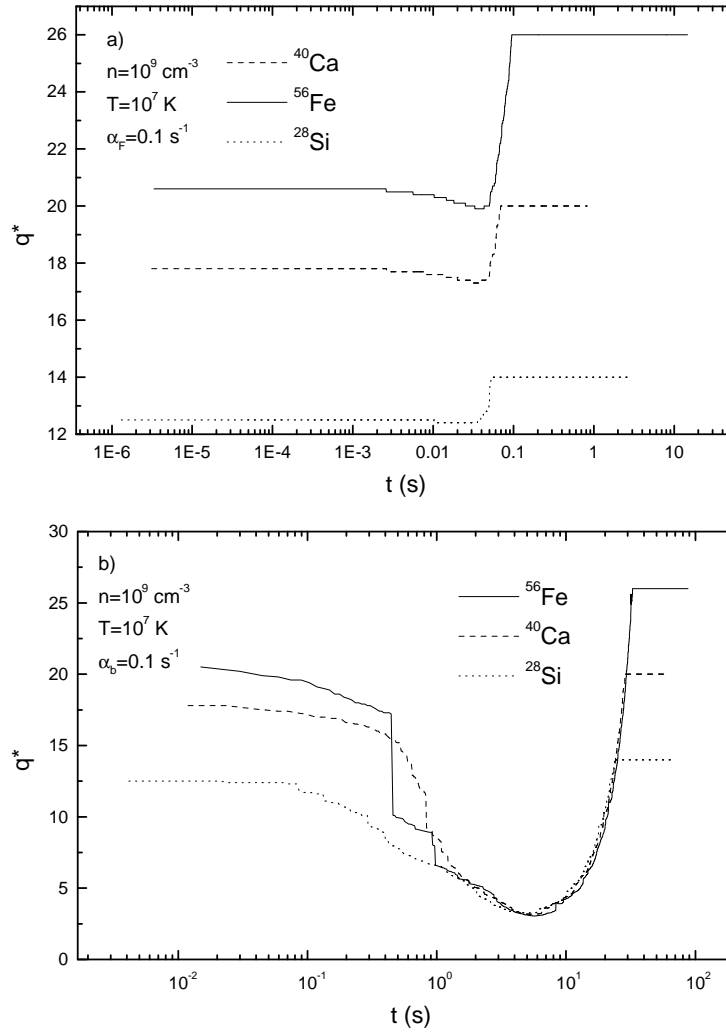


**Figure 3.** Temporal evolution of the effective charge,  $q^*$ , of  $^{56}\text{Fe}$ ,  $^{40}\text{Ca}$  and  $^{28}\text{Si}$  fast ions against the trapping time in the acceleration region under Fermi (a) and betatron (b) acceleration mechanisms with  $0.1 \text{ s}^{-1}$  acceleration efficiency in a  $10^7 \text{ K}$  hot plasma and  $10^9 \text{ cm}^{-3}$  density number.

#### 4. Conclusions

The behaviour of the charge state evolution of cosmic rays has been analysed during their acceleration in solar flares, where the targets' thermal velocities have been implemented in the charge exchange cross sections. From the achieved results, it is observed that at the first step, when the ions undergo acceleration they are disturbed from their thermal equilibrium in the plasma, where they present a particular charge state. When the acceleration rate is high, there seems to not be enough time for the thermal equilibrium between the ion and the ambient plasma to set in. What is more, the ion responds to charge exchange processes instead of ionization by thermal equilibrium. In general terms, it can be summarized that the ion starts its acceleration by capturing electrons, then its charge diminishes quickly reaching a minimum value. In addition, it will lose electrons as it accelerates. Finally, the process will cease when

the particle is liberated from the source with a specific effective charge and kinetic energy.

Comparing the behaviour of the charge states obtained here, with those predicted by the effective charge semi-empirical equation of Barkas–Blume, we can state that in general, this equation overestimates the ion charge at low energies and underestimates it for high energies, as can be observed in figure 1.

Other conclusive evidence was obtained when betatron and Fermi acceleration mechanisms were compared. The Fermi acceleration mechanism energizes the ions faster than the betatron does. Consequently, the ion captures more electrons while it is accelerated by the betatron mechanism, as can be observed in figure 2. Hence, the betatron mechanism is less effective at accelerating ions, and higher efficiencies are required to obtain results similar to those secured with the Fermi mechanism. In addition, since more electrons are captured the thermal effective charge of the particle must be higher, which necessarily ought to equal the plasma's temperature in the acceleration region.

Finally, we have to point out that differences in the charge state of the solar energetic particles can be expected from one solar flare to another, depending on the trapping time, the acceleration mechanism acting, its efficiency, and the physical characteristics of the source, whether it be the density number or the temperature.

### Acknowledgments

The initial stage of this work was performed in the Instituto de Geofísica (UNAM), during the postdoctoral positions of the first two authors. They wish to acknowledge the Instituto de Geofísica for these postdoctoral contracts which have permitted the first-stage development of this work.

### References

- [1] Sciambi R K, Gloeckler G, Fan C Y and Hovestadt D 1977 *Astrophys. J.* **214** 316
- [2] O'gallagher J J *et al* 1976 *Astrophys. J. Lett.* **209** L97
- [3] Gloeckler G, Sciambi R K, Fan C Y and Hovestadt D 1976 *Astrophys. J. Lett.* **209** L93
- [4] Crawford H J, Price P B, Cartwright B G and Sullivan J D 1975 *Astrophys. J.* **195** 213
- [5] Bethe J and Salpeter 1957 *Quantum Mechanics of One and Two Electron Systems* (Berlin: Springer) pp 320–2
- [6] Nikolaev V S 1965 *Sov. Phys.–Usp.* **8** 269
- [7] Burgess A 1965 *Astrophys. J.* **141** 1588
- [8] Arnaud M and Rothenflug R 1985 *Astron. Astrophys. Suppl.* **60** 425
- [9] Perez-Peraza J, Martinell J and Villareal A 1982 *Adv. Space Res.* **2** 197
- [10] Perez-Peraza J and R Lara A 1979 *Proc. 16th Int. Cosmic Ray Conf. (Kyoto, Japan, Aug. 1979)* vol 12, pp 259–364